0090-9556/10/3810-1747–1759$20.00
DRUG METABOLISM AND DISPOSITION
Vol. 38, No. 10
33373/3625798
DMD 38:1747–1759, 2010
Printed in U.S.A.

Development of a Systematic Approach to Identify Metabolites for Herbal Homologs Based on Liquid Chromatography Hybrid Ion Trap Time-of-Flight Mass Spectrometry: Gender-Related Difference in Metabolism of *Schisandra* Lignans in Rats[S]

Yan Liang, Haiping Hao, Lin Xie, An Kang, Tong Xie, Xiao Zheng, Chen Dai, Kun Hao, Longsheng Sheng, and Guangji Wang

Key Laboratory of Drug Metabolism and Pharmacokinetics, China Pharmaceutical University, Nanjing, People's Republic of China

Received March 18, 2010; accepted July 13, 2010

ABSTRACT:

Metabolic research for herbal medicine (HM) is a formidable task, which is still in its infancy due to complicated components in HM, complex metabolic pathways, and lack of authentic standards. The present work contributes to the development of a powerful technical platform to rapidly identify and classify metabolites of herbal components based on a liquid chromatography hybrid ion trap time-of-flight mass spectrometry. Taking *Schisandra* lignans extract as an example, the metabolic studies were completed both in vitro and in vivo. In the in vitro study, metabolites for five representative *Schisandra* lignans were identified and structurally characterized. The major metabolic pathways were summed as demethylation, hydroxylation, and demethylation and hydroxylation. In the in vivo study, 44 metabolites were detected in rat urine. These metabolites were identified and classified rapidly according to the metabolic rules obtained in the in vitro studies, and hydroxylation was confirmed as the primacy metabolic pathway for lignans in rat urine. In addition, "relative cumulative excretion" (RCE) for the metabolites in female and male rats were calculated according to their relative intensities in the urine samples collected at 0 to 12, 12 to 24, and 24 to 36 h. As a result, great gender-related difference on RCE was observed. For most metabolites, RCE in female rats was significantly lower than that in male rats. In conclusion, the presently developed methodology and approach on metabolic research for *Schisandra* lignans will find its wide use in metabolic studies for herbal medicines.

Introduction

Herbal medicines (HMs) have been used for more than 2000 years, most likely because they are able to control complex disease systems with little expense (Goldrosen and Straus, 2004; Curiati et al., 2005). Yet, it is essential to conduct scientific evaluation of pharmacokinetics and biotransformation of HMs to use them in a greater role in the treatment of various diseases (Engel and Straus, 2002; Goldrosen and Straus, 2004). Metabolic study is crucial in clarifying how active constituents produce the effectiveness of the HM, yet HMs are complex and it is often difficult to determine which component is the active constituent. Furthermore, lacking standards is another challenge in assessing the biotransformation for the constituents in HMs (Huang et al., 2004; Yang et al., 2009; Jiang et al., 2010).

More recently, high-performance liquid chromatography (HPLC) has been coupled with various mass spectrometry (MS) detectors for analysis of multicomponents in complex medium. Among them, the newly developed hybrid ion trap and time-of-flight mass spectrometry (IT-TOF/MS) was selected for its unmatched sensitivity, accuracy, resolution, and high throughput for the identification of complex compounds in addition to its excellent MS^n function (Hao et al., 2008; Zheng et al., 2009). Liquid chromatography-hybrid ion trap and time-of-flight mass spectrometry (LC-IT-TOF/MS) has been successfully applied to the global identification of target and nontarget components in Shengmai and Mai-Luo-Ning injection, as well as identification of several drug metabolites (Hao et al., 2008; Wang et al., 2009; Zheng et al., 2009).

In the present study, a convincible and generally applicable approach was proposed to identify metabolites of HM based on LC-IT-TOF/MS. Such a strategy was developed from a concept that com-

This work was supported in part by the National Natural Science Foundation of China [Grants 30801422, 30630076]; the Natural Science Foundation of Jiangsu Province [Grant BK2008038]; and the National Key New Drug Creation Special Programme [Grants 2009ZX09304-001, 2009ZX09502-004].

Y.L. and H.H. contributed equally to this work.

Article, publication date, and citation information can be found at http://dmd.aspetjournals.org.

doi:10.1124/dmd.110.033373.

[S] The online version of this article (available at http://dmd.aspetjournals.org) contains supplemental material.

ABBREVIATIONS: HM, herbal medicine; HPLC, high-performance liquid chromatography; MS, mass spectrometry; IT-TOF/MS, hybrid ion trap and time-of-flight mass spectrometry; LC-IT-TOF/MS, liquid chromatography-hybrid ion trap and time-of-flight mass spectrometry; SLE, *Schisandra* lignans extract; RCE, relative cumulative excretion; EICs, extracted ion chromatograms; LC-ESI-IT-TOF/MS, liquid chromatography electrospray ionization hybrid ion trap and time-of-flight mass spectrometry; GEM, gradient elution mode; CID, collision-induced dissociation; UDPGA, UDP-glucuronic acid; P450, cytochromes P450.

pounds with similar structures have similar metabolic rules, and the metabolism in vitro can be used to predict the metabolic pathways in vivo to some extent (Vickers et al., 1993; Vanden et al., 1998). Moreover, liver S9 and intestinal S9 fractions can be used as the major tools for studying xenobiotic metabolism in vitro due to the high expression of drug-metabolizing enzymes, including the cytochromes P450, flavin monooxygenases, and UDP-glucuronyl transferases (Mori et al., 1986; Masaki et al., 2007). Based on the knowledge above, the proposed strategy involves four procedural steps: 1) qualitative analysis of the constituents in HM; 2) in vitro study to identify the metabolites in liver S9/intestinal S9 for representative standards one by one, and summing their metabolic rules; 3) in vivo study to determine the constituents by comparing the profiling of blank and dosed urine, feces, bile etc., and seeking metabolites by comparing the components in HMs and dosed samples; 4) tracing the source of metabolites in vivo for HMs according to the metabolic rules of standards obtained in step 2.

To test this procedure, we used *Schisandra* lignans extract (SLE). SLE is a well known herbal medicine that possesses several beneficial pharmacological effects, including antihepatotoxic, antiasthmatic, antigastric ulcer, potent antioxidative properties, detoxification, and anticarcinogenic activity (Deng et al., 2008; Xu et al., 2008). *Schisandra* lignans are major active compounds of *Schisandra chinensis*, and metabolism of *Schisandra* lignans in vitro and in vivo plays an important role in explaining and predicting efficacy and toxicity for the parent compounds. We have previously detected and structurally characterized 20 kinds of *Schisandra* lignans from Shengmai injection, using a diagnostic fragment-ion-based extension strategy (Zheng et al., 2010). Afterward, such a strategy was applied for characterizing the lignans components in SLE, and 31 lignans were identified and structurally characterized as shown in Fig. 1. We confirmed schizandrol A and B, schizandrin A and B, and schisantherin A as the major constituents in SLE. Herein, the metabolism of these five major lignans had been studied in rat liver and intestinal S9 systems, respectively. Their metabolic rules were used to identify and classify metabolites in rat urine rapidly and conveniently. Moreover, a "relative cumulative excretion" (RCE), calculated according to the peak area of extracted ion chromatograms (EICs) from acquisition data, was developed to assess gender difference independent of specific authentic compounds for each metabolite.

Materials and Methods

Chemicals and Reagents. Schizandrol A and B, schizandrin A and B, and schisantherin A (>98% purity) were purchased from Sichuan Weikeqi Bio-Technology Co., Ltd. (Chengdu, China). SLE was purchased from Nanjing Qingze Medical Technological Development Co. Ltd. (Nanjing, China) (constituents shown in Fig. 1). Glucose-6-phosphate dehydrogenase, monosodium D-glucose 6-phosphate, and NADPH were purchased from Sigma-Aldrich (St. Louis, MO). HPLC-grade methanol was purchased from Thermo Fisher Scientific (Waltham, MA). Water was collected from a Milli-Q Ultrapure water system with the water outlet was operating at 18.2 MΩ (Millipore Corporation, Billerica, MA). Other chemicals and solvents were all of analytical grade.

Preparation of Rat Liver and Intestinal S9. Six female and six male Sprague-Dawley rats weighing 200 ± 20 g were purchased from the Laboratory Animal Center of Peking University Health Science Center (Beijing,

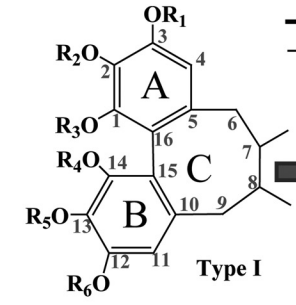

Type I	R1	R2	R3	R4	R5	R6
Gomisin T-ol	OH	CH3	CH3	CH3	CH3	CH3
Gomisin J	H	CH3	CH3	CH3	CH3	CH3
Gomisin K1	H	CH3	CH3	CH3	CH3	CH3
Gomisin M1	-CH2-		CH3	H	CH3	CH3
Gomisin M2	-CH2-		H	CH3	CH3	CH3
Gomisin L1	CH3	CH3	H	CH3	-CH2-	
Gomisin L2	H	CH3	CH3	CH3	-CH2-	
Schizandrin A	CH3	CH3	CH3	CH3	CH3	CH3
γ -Schizandrin	-CH2-		CH3	CH3	CH3	CH3
Schizandrin B	CH3	CH3	CH3	CH3	-CH2-	

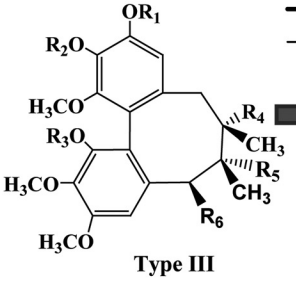

Type III	R1	R2	R3	R4	R5	R6
Gomisin G1	-CH2-		CH3	H	OH	OBz
Gomisin H	CH3	CH3	H	OH	H	H
Gomisin	H	CH3	CH3	H	H	OH
Tigolygomisin H	CH3	CH3	-OTig	OH	H	H
Angelygomisin H	CH3	CH3	-OAng	OH	H	H
Tigolygomisin P	-CH2-		CH3	H	OH	-OTig
Angelygomisin P	-CH2-		CH3	H	OH	-OAng

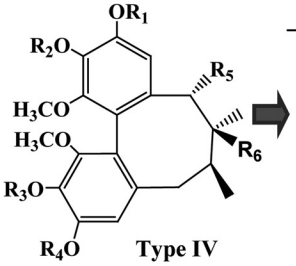

Type IV	R1	R2	R3	R4	R5	R6
Schisantherin B	CH3	CH3	-CH2-		-OAng	OH
Gomisin G	-CH2-		CH3	CH3	-OBz	OH
Schisantherin A	CH3	CH3	-CH2-		-OBz	OH
Angelygomisin Q	CH3	CH3	CH3	CH3	-OAng	OH
Gomisin R	-CH2-		-CH2-		OH	H
Schisantherin C	CH3	CH3	-CH2-		-OTig	OH
Gomisin F	-CH2-		CH3	CH3	-OAng	OH

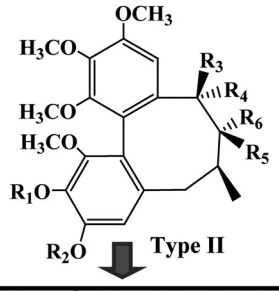

Type II	R1	R2	R3	R4	R5
Schizandrol A	CH3	CH3	H	H	OH
Schizandrol B	-CH2-		H	H	OH
Gomisin O	-CH2-		H	OH	H
Epigomisin O	-CH2-		OH	H	H

Type IV	R1	R2
Gomisin D	OH	CH3

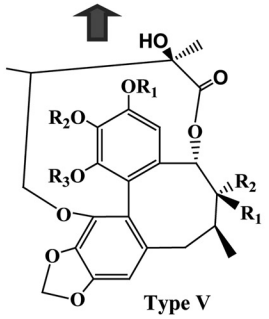

FIG. 1. Structures of *Schisandra* lignans in SLE.

People's Republic of China) and kept in an environmentally controlled breeding room for at least 3 days before experimentation. The rats were fed with standard laboratory food and water and fasted overnight but with free access to water before the test. Animal welfare and experimental procedures were strictly in accordance with the guide for the care and use of laboratory animals (Institute of Laboratory Animal Resources, 1996) and the related ethical regulations of our university. The rats were sacrificed by exsanguination from the abdominal aorta under ether anesthesia. Liver S9 fractions were prepared using established procedures (Mori et al., 1986) with slight improvement. The procedure is briefly described as follows: The rat livers were blotted dry, weighed, and mixed with 70 mM H_2PO_4 buffer solution at a ratio of 1 g liver/2 ml of buffer solution. The liver was homogenized by mixing for two 30-s periods at high speed, using a Mixmate Mixer (Eppendorf North America, Waterbury, NY). The homogenized liver was then centrifuged at 4°C for 30 min at 9000*g* (Eppendorf North America). Aliquots of the resulting supernatant were placed in several polypropylene tubes and stored frozen at −80°C. Protein contents were determined by the method of Bradford (1976) using bovine serum albumin as the standard.

Intestinal S9 fractions were prepared as described previously (Masaki et al., 2007). In brief, the intestine was cut longitudinally and the mucosa was removed by gently scraping the inside surface with a metal spatula. Homogenization was performed with a Potter-Elvehjelm homogenizer in ice-cold 50 mM Tris-HCl buffer, pH 7.8, containing 0.25 M sucrose, 0.5 mM EDTA, and 40 μg of phenylmethylsulphonyl fluoride/ml. Subsequently, centrifugation at 9750*g* for 20 min was used to obtain a supernatant fraction containing the cytosol and microsomal fraction, designated the S9 fraction.

Incubations with NADPH in S9 Systems. Ten microliters of schizandrol A and B, schizandrin A and B, and schisantherin A (20 μM) were incubated with 20 μl of rat liver/intestinal S9 (1 mg/ml) in a medium containing potassium phosphate buffer (0.1 M, pH 7.4) and 10 mM $MgCl_2$ (20 μl). Reactions were initiated by addition of the NADPH-generating system, resulting in a final concentration of 10 mM monosodium D-glucose 6-phosphate, 0.5 mM NADPH, and 1 unit/ml glucose-6-phosphate dehydrogenase, and final volume of the reaction mixture was 200 μl. The incubations were carried out at 37°C in a shaking water bath. Control incubations without the NADPH-generating system were performed under the same conditions. The reactions were terminated by the addition of ice-cold acetonitrile (200 μl). Precipitated materials were removed by centrifugation at 40,000*g* for 10 min at 4°C, and the supernatants were collected for liquid chromatography ionization hybrid ion trap and time-of-flight mass spectrometry (LC-ESI-IT-TOF/MS) analysis.

Drug Administration and Urine Sampling. To collect urine samples, five male rats and five female rats were housed in Nalgene metabolic cages (one rat per cage) and received oral SLE at 500 mg/kg (via gavage). Urine samples were collected from three rats at 0 to 12, 12 to 24, and 24 to 36 h after dosing. All samples were stored at −20°C until analysis. Solid-phase extraction with a C18 cartridge was used to purify the urine samples. Before extraction, the cartridge was conditioned with 1 ml of methanol followed by 1 ml of water. During the sample passing through the cartridge, 2 ml of water was added to remove the impurity. Then, the analytes adsorbed on the stationary phase were eluted by 1 ml of methanol. The methanol effluent was centrifuged at 40,000 rpm for 10 min at 4°C, and 5 μl of supernatant was injected into the LC-IT-TOF/MS system.

Liquid Chromatography to Determine *Schisandra* Lignans. LC experiments were conducted on a HPLC system consisting of an LC-20AD binary pump, DGU-14A degasser, SIL-20AD autosampler, and a CTO-20AC column oven (Shimadu, Kyoto, Japan). Chromatographic separation was achieved on a SymmetryShield RP8 column (3.5 μm, 50 × 2.1 mm i.d.; Waters, Milford, MA) at 40°C. The mobile phase (delivered at 0.2 ml/min) consisted of solvent A, CH_3OH/H_2O (5:95, v/v, containing 1.0 μM NaAc) and solvent B, CH_3OH/H_2O (95:5, v/v, containing 1.0 μM NaAc). To indentify the metabolites of the five major *Schisandra* lignans in S9 systems rapidly, and to isolate the parent components and metabolites of SLE in rat urine effectively, two gradient elution modes (GEMs) were carried in this study. For GEM1: initial 60% B for 6.0 min, linear gradient 60 to 90% B from 6.0 to 8.0 min and maintained for 3 min, then quickly returned to initial 60% B and maintained until 15 min for column balance. For GEM2: initial 55% B for 0.2 min, linear gradient 55 to 65% B from 0.2 to 25.0 min and 65 to 85% B from 25.0 to 40.0 min, then quickly returned to initial 55% B and maintained until 48 min for column balance.

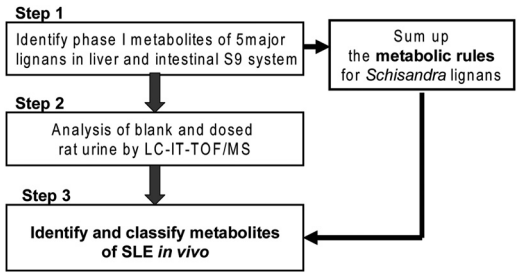

FIG. 2. Systematic workflow.

ESI-IT-TOF Mass Spectrometry. The mass spectrometer of LC-IT-TOF/MS (Shimadzu, Kyoto, Japan) was equipped with an ESI source in positive ion mode at a full width at half maximum. The optimized analytical conditions were as follows: detector voltage, 1.60 kV; nebulizing gas (N_2) flow, 1.5 l/min; dry gas (N_2) flow, 50 kPa; scan range, *m/z* 350 to 800 for MS^1, 100 to 600 for MS^2, and 50 to 500 for MS^3; ultrahigh purity argon was used as the collision gas for collision-induced dissociation (CID) experiments, and the collision energy was set at 50% for MS^2 and 100% for MS^3; pressure of TOF region, 1.5×10^{-4} Pa; ion trap pressure, 1.7×10^{-2} Pa; ion accumulated time, 50 ms; precursor ion selected width, 3.0 amu. Accurate mass determination was corrected by calibration using the sodium trifluoroacetate clusters as reference. Shimadzu's Composition Formula Predictor software was used to verify identifications for *Schisandra* lignans.

Systematic Workflow. The systematic workflow is schematically depicted in Fig. 2. In step 1, the phase I metabolites in liver S9 for the major lignans (schizandrol A and B, schizandrin A and B, and schisantherin A) were identified and structurally characterized based on the accurate MS and MS^n measured by LC-ESI-IT-TOF/MS, and the metabolic rules were summed for the *Schisandra* lignans. In step 2, we identified the metabolites in intestinal S9 for the five major lignans and tried to sum up the metabolic rules for *Schisandra* lignans. In step 3, we analyzed blank and dosed rat urine using LC-IT-TOF/MS and picked up all the constituents that only appeared in dosed samples, and then we compared data between the blank and dosed rat using Profiling Solution software; in step 4, we searched for metabolites by comparing the components in SLE and dosed samples; we then inferred the source of metabolites based on the metabolic rules summed in steps 1 and 2.

Results

Phase I Metabolites of Five Major Lignans in Female and Male Liver S9 Systems (Step 1). Schizandrol A and B, schizandrin A and B, and schisantherin A (20 μM) were incubated in both the presence and absence of the NADPH-generating system with female and male rat liver S9 fractions one by one. The LC separation was carried out under GEM1 mode, and the eluate from HPLC was analyzed by IT-TOF mass spectrometer. Targeted data analysis was carried out with the aid of MetID solution software, which uses an extensive list of potential biotransformation reactions (e.g., methylation, hydroxylation, demethylation, etc.), in conjunction with the elemental compositions of the parent molecules, to generate a series of EICs from acquisition data sets of MS. All of the selected precursor ions were subjected to up to MS^3 experiments, and two collision energies at 50 and 100% were applied to all precursor ion fragmentations to generate sufficient product ions effectively. The MS^n spectra of all the metabolites of schizandrol A and B, schizandrin A and B, and schisantherin A had been shown in Supplemental Fig. 1, and the relevant results (retention time, formula, accurate mass, mass error, fragment ions and so on) are listed in Table 1.

The fragment pathways of parent compounds were proposed according to the accurate MS^n data to facilitate metabolite identification. Taking schizandrol A as an example, the product ions at *m/z* 440.1765

TABLE 1

Retention time, formula, accurate mass, mass error, fragment ions, biotransformation, and peak area of five lignans and their metabolites in female and male rat liver S9 detected by LC-IT-TOF/MS

	Mets	t_R (min)	*m/z* $[M + Na]^+$	Formula	Error (ppm)	Fragment Ions (*m/z*)
Schizandrol A	I-M0	8.95	455.2040	$C_{24}H_{32}O_7$	0.0	237.1097; 241.1037; 273.1213; 295.1509; 409.1675; 410.1763; 415.2109; 423.1441; 440.1765
	I-M1	6.26	457.1828	$C_{23}H_{30}O_8$	−0.5	442.1593; 439.1759; 411.1427
	I-M2	7.01	441.1868	$C_{23}H_{30}O_7$	−1.6	401.1985; 369.1689
	I-M3	7.88	471.1985	$C_{24}H_{32}O_8$	−0.4	273.1213; 295.1509; 425.1583; 426.1609; 453.1970; 456.1724
	I-M4	8.14	441.1875	$C_{23}H_{30}O_7$	−0.9	395.1479; 369.1689
Schizandrol B	II-M0	9.57	439.172	$C_{23}H_{28}O_7$	−0.7	393.1298; 394.1321; 399.1724; 424.1540
	II-M1	7.18	425.1567	$C_{22}H_{26}O_7$	−0.4	410.1342; 385.1537; 369.1689; 277.1442
	II-M2	7.16	441.1504	$C_{22}H_{26}O_8$	−1.6	426.1346; 423.1446; 277.1439
	II-M3	7.51	441.1504	$C_{22}H_{26}O_8$	−1.6	426.1346; 423.1446; 277.1439
	II-M4	8.72	455.1672	$C_{23}H_{28}O_8$	−0.4	440.1477; 437.1611; 410.1493; 409.1278
	II-M5	8.94	425.1572	$C_{22}H_{26}O_7$	0.1	410.1342; 369.1689; 277.1439
	II-M6	9.17	425.1556	$C_{22}H_{26}O_7$	−1.5	365.1950; 262.1357; 225.0974
Schisantherin A	III-M0	10.05	559.1922	$C_{30}H_{32}O_9$	−1.7	437.1561; 415.1727; 385.1615; 371.1457; 391.1004
	III-M1	8.47	545.1764	$C_{29}H_{30}O_9$	−1.8	423.1416; 401.1519; 391.1247; 392.1274; 377.0978
	III-M2	8.73	575.1845	$C_{30}H_{32}O_{10}$	−4.3	437.1567; 391.1726; 385.1669; 371.1489; 341.1288
	III-M3	9.24	575.1863	$C_{30}H_{32}O_{10}$	−2.5	437.1567; 391.1726; 385.1669; 371.1489; 341.1288
	III-M4	9.61	545.1771	$C_{29}H_{30}O_9$	−1.1	423.1462; 359.1452; 491.1803; 253.1312
Schitherdrin	IV-M0	10.47	439.2067	$C_{24}H_{32}O_6$	−2.4	393.1669; 424.1858
	IV-M1	6.14	471.1973	$C_{24}H_{32}O_8$	−1.6	441.1721
	IV-M2	6.31	457.1817	$C_{23}H_{30}O_8$	−1.6	442.1593; 439.1759; 293.1427
	IV-M3	7.10	441.1888	$C_{23}H_{30}O_7$	0.4	369.1323; 395.1456; 426.1669
	IV-M4	7.88	471.1947	$C_{24}H_{32}O_8$	−4.2	273.1213; 295.1509; 425.1583; 426.1609; 453.1970; 441.1721; 456.1724
	IV-M5	7.70	441.1888	$C_{23}H_{30}O_7$	0.4	369.1323; 395.1456; 426.1669
	IV-M6	8.95	455.2042	$C_{23}H_{30}O_7$	−0.0	440.1768; 410.1610; 409.1608; 295.1509
	IV-M7	10.06	425.1900	$C_{23}H_{30}O_6$	−3.5	371.1879; 339.1532; 301.1036; 343.1887; 339.1570
Schitherdrin B	V-M0	10.80	423.1743	$C_{23}H_{28}O_6$	−3.5	386.1689; 371.1858; 340.1598; 331.1198; 300.1002
	V-M1	7.36	453.1873	$C_{24}H_{30}O_7$	−1.1	433.2008
	V-M2	7.73	425.1568	$C_{22}H_{26}O_7$	−2.7	410.1342; 385.1537; 369.1689
	V-M3	7.86	453.1873	$C_{24}H_{30}O_7$	−1.1	319.1054
	V-M4	9.39	439.1717	$C_{23}H_{28}O_7$	−1	359.1826
	V-M5	9.53	409.1615	$C_{22}H_{26}O_6$	−0.7	355.1536; 325.1422; 317.0954; 287.0826; 285.0841; 269.1058
	V-M6	10.40	409.1616	$C_{22}H_{26}O_6$	−0.6	381.1679; 378.1491; 363.1179; 365.1303; 355.1496; 317.1031; 285.1460; 235.1295

and 409.1675 (loss of CH_3 and C_2H_6O, respectively) were abundant in the ESI-MS^2 data of the $[M+Na]^+$ ion at *m/z* 455.2040, and peaks at *m/z* 415.2109 (loss of H_2O) and 410.1763 (loss of C_2H_5O) were also found in this process. In the ESI-MS^3 experiment of the *m/z* 440.1765 ion, the product ion was observed at *m/z* 295.1509 corresponding to the elimination of $C_6H_3O_3$, and the fragment ion at *m/z* 273.1213 corresponding to the elimination of $C_6H_8O_2$ was found in the ESI-MS^3 data of the *m/z* 409.1675, then the fragmentation pathway could be predicted, as shown Supplemental Fig. 2). In addition, the proposed fragmentation pathways of schizandrol B, schizandrin A and B, and schisantherin A are also listed in Supplemental Fig. 2.

When schizandrol A ($C_{24}H_{32}O_7$) was incubated with female rat liver S9 in presence of NADPH, four major suspected phase I metabolites were found with the aid of MetID solution software. The EICs of schizandrol A and its possible metabolites are shown in Fig. 3A. No metabolite was detected in the absence of the NADPH-generating system. The major metabolite was I-M3, which was calculated as $C_{24}H_{32}O_8$ by the Formula Predictor software according to the determined accurate mass. Thus, I-M3 (addition of O) was preliminarily elucidated as the hydroxylation product of schizandrol A. To pinpoint the site of hydroxylation in this metabolite, we compared the MS^n data from I-M3 with the corresponding data of the parent drug. The fragment obtained from the precursor (*m/z* 471.1985) showed major product ions at *m/z* 456.1724 and 425.1583, which could lead to MS^3 product ions at *m/z* 295.1509 and 273.1213, respectively. On the basis of the elemental compositions of fragment ions and structure of the parent molecule, the most likely hydroxylation position was located at C-4 of A ring, and the possible structure and proposed fragmentation pathways of I-M3 were shown in Fig. 3E. The results also demonstrated that the hydroxylation was the predominant metabolic pathway of schizandrol A in female rat liver S9. In addition, two demethylation metabolites (I-M2 and I-M4) and a demethylation-hydroxylation metabolite (I-M1) were found in this system by comparison with schizandrol A, and the locations of reactions were concluded based on their proposed fragmentation pathways (as shown in Fig. 3). In contrast, only two metabolites (I-M1 and I-M4) were found when schizandrol A was incubated with male rat liver S9 in presence of NADPH (see Fig. 3B). The major metabolite was I-M1, whereas I-M4 was produced at levels close to the lowest limit of detection.

When schizandrol B ($C_{23}H_{28}O_7$) was incubated with female and male rat liver S9 and NADPH, six metabolites were identified by comparing the mass profiling with that of incubation system without NADPH. From the EICs of schizandrol B and its metabolites in female and male rat liver S9 (Fig. 4, A and B), we could find that II-M4 was the major metabolite, and the intensity of II-M4 in male rat liver S9 was much higher than that in female rat liver S9. Likewise, the intensities of II-M2 and II-M3 in male rat liver S9 were also higher than that in female. As expected, the peak area of schizandrol B in female rat liver was 3-fold larger than that in the male. The types of metabolic reactions were deduced as demethylation (II-M1, II-M5, and II-M6), hydroxylation (II-M4), and demethylation-hydroxylation (II-M1 and II-M5), respectively. Structural characterization for these metabolites was completed based on their proposed fragmentation pathways (as shown in Fig. 4, C–H).

After schisantherin A ($C_{30}H_{32}O_9$) was incubated with rat liver S9 in presence of NADPH, four major suspected metabolites were found in male rat liver S9 with the aid of MetID solution software. III-M2, one of the hydroxylation metabolites, was a male rat-specific metabolite

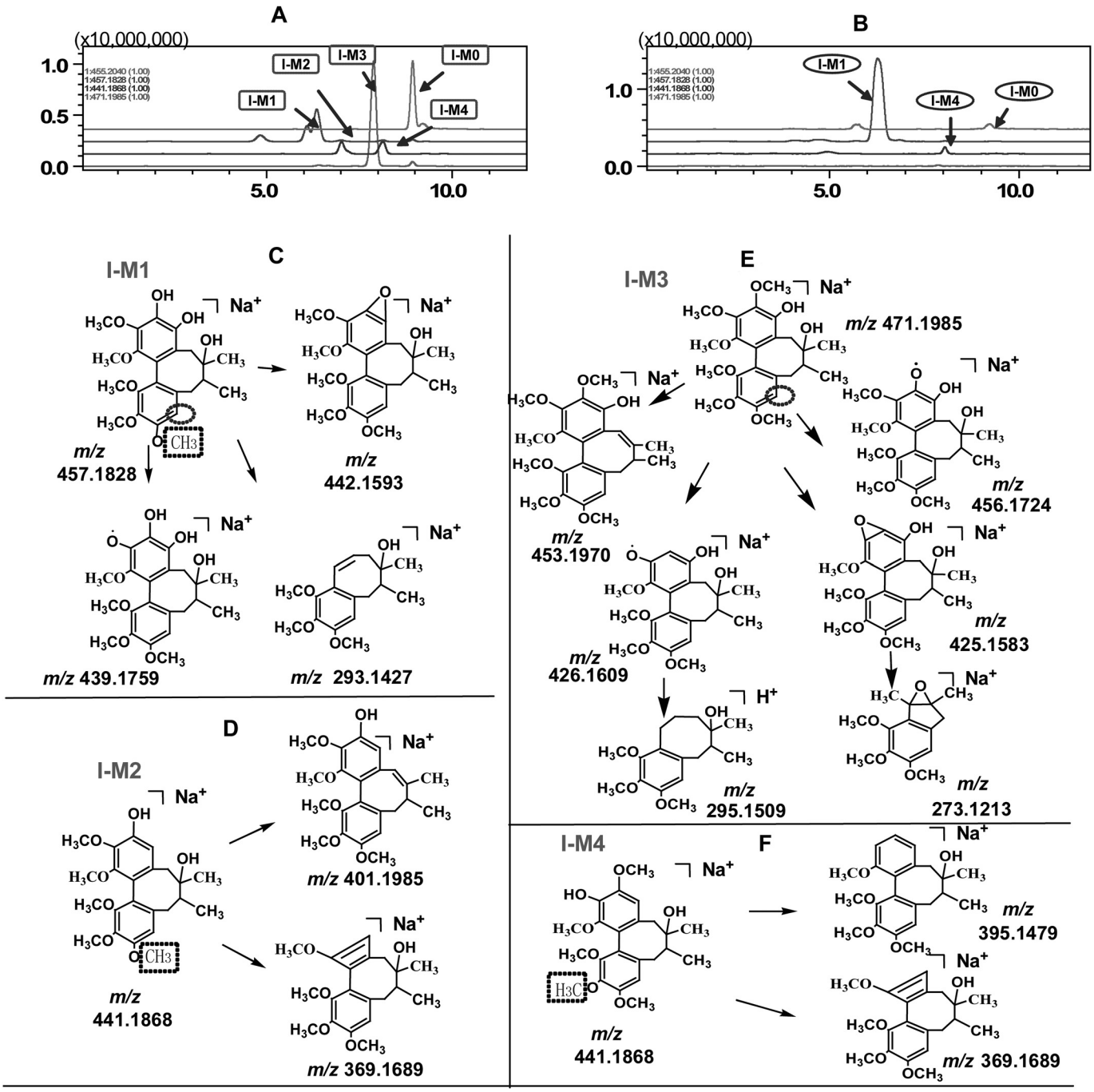

FIG. 3. EICs of schizandrol A and their metabolites in female (A) and male (B) rat liver S9 in the presence of NADPH measured by LC-IT-TOF/MS, and the fragmentation pathways of the possible metabolites of schizandrol A (C–F). Dotted square: the potential demethylation site; dotted circle: the potential hydroxylation site.

and could not be detected in female rat liver S9 in presence of NADPH. The EICs of schisantherin A and its possible metabolites produced in female and male rat liver S9 are shown in Fig. 5, A and B, respectively. III-M1 and III-M4, characterized with similar sodium adduct ion at *m/z* 545.1769 and *m/z* 545.1771 and same predicted elemental composition of $C_{29}H_{30}O_9$, suggested that they were the demethylation product at different methoxy groups. The further fragmentation patterns and retention behavior analysis helped us to determine the demethylation positions for III-M1 and III-M4 (see Fig. 5, C and F). In addition, III-M2 and III-M3, eluted at 8.73 and 9.24 min, showed major sodium adduct ion at *m/z* 575.1855 and *m/z* 575.1863. They were both tentatively presumed to be the hydroxylation metabolites of schisantherin A according to their predicted elemental composition of $C_{30}H_{32}O_{10}$. The fragment ion of III-M2 and III-M3 at *m/z* 437.1567, which is the same as the major fragment ion of the schisantherin A produced by loss of the OBz group, supported the fact that the hydroxylation position should be located at the OBz group. The retention behavior analysis was also helpful to the structural characterization for III-M2 and III-M3, and the results were shown in Fig. 5, D and E, clearly.

Several metabolites, principally hydroxylation (IV-M1, IV-M4, and IV-M6), demethylation (IV-M7), and demethylation-hydroxylation (IV-M3 and IV-M5) metabolites, were identified according to their accurate mass measurement when schizandrin A was incubated with

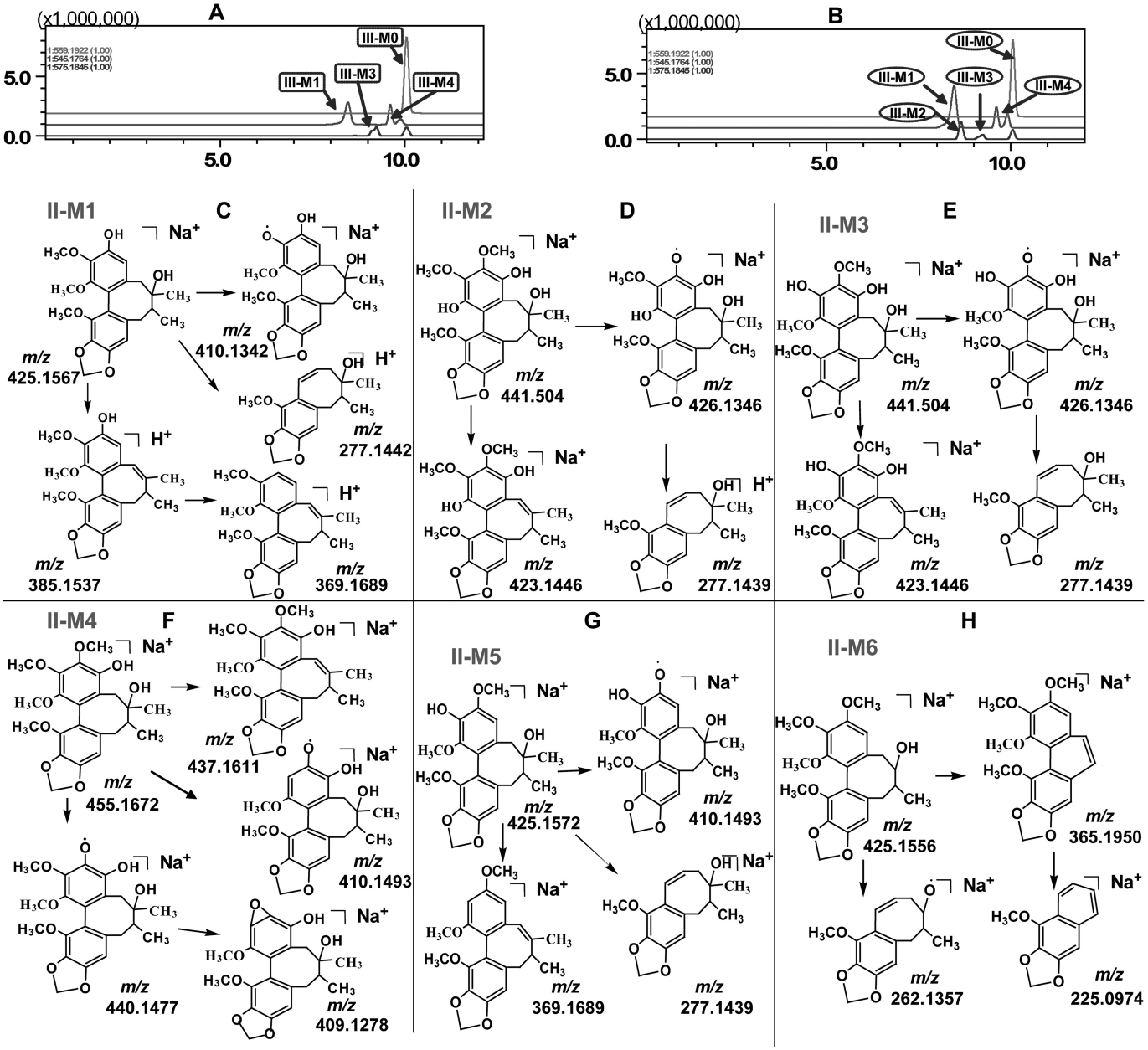

FIG. 4. EICs of schizandrol B and their metabolites in female (A) and male (B) rat liver S9 in the presence of NADPH measured by LC-IT-TOF/MS, and the fragmentation pathways of the possible metabolites of schizandrol B (C–H).

female rat liver S9 in the presence of NADPH. In addition, the EICs of schizandrin A and its metabolites in female and male rat liver S9 system were shown in Fig. 6, A and B. IV-M4 and IV-M7 were female rat-specific metabolites and could only be produced under the catalysis of the NADPH-independent female S9 enzymes. IV-M2, a demethylation-hydroxylation metabolite, was only detected in the male rat liver S9 system. As a result, gender difference on the metabolites and schizandrin A was obvious, and the peak area of schizandrin A in female rat liver was 6.5-fold larger than that in male. The procedure of structural characterization for these seven metabolites is shown in Fig. 6, C–H.

After incubating schizandrin B ($C_{23}H_{28}O_6$) with rat liver S9 system supplemented with NADPH, six metabolites were identified with the aid of MetID solution software. The EICs of schizandrin B and its metabolites in female and male rat liver S9 system are shown in Fig. 7, A and B, respectively. Great gender difference was found easily because the intensities of these metabolites produced in male rat liver S9 system was much higher than that produced in female rat liver S9. As expected, the peak area of schizandrin B in female rat liver S9 system was 13-fold larger than that in male. V-M1 and V-M3, characterized with same sodium adduct ion at *m/z* 453.1873 and predicted elemental composition of $C_{24}H_{30}O_7$, suggested that they were the demethylation and hydroxylation product at different positions. V-M2 (*m/z* 425.1568, $C_{22}H_{26}O_7$) was proposed as a demethylation-hydroxylation metabolite. V-M4 (*m/z* 439.1717), eluted at 9.39 min, was tentatively presumed to be the hydroxylation metabolites of schizandrin B according to their predicted elemental composition ($C_{23}H_{28}O_7$). V-M5 and V-M6, which showed major sodium adduct ion at *m/z* 409.1615 and *m/z* 409.1616 and the same predicted elemental composition of $C_{22}H_{26}O_6$, were both deduced as the demethylation metabolites of schizandrin B. Then, the locations of reactions were concluded based on their proposed fragmentation pathways (as shown in Fig. 7, C and G).

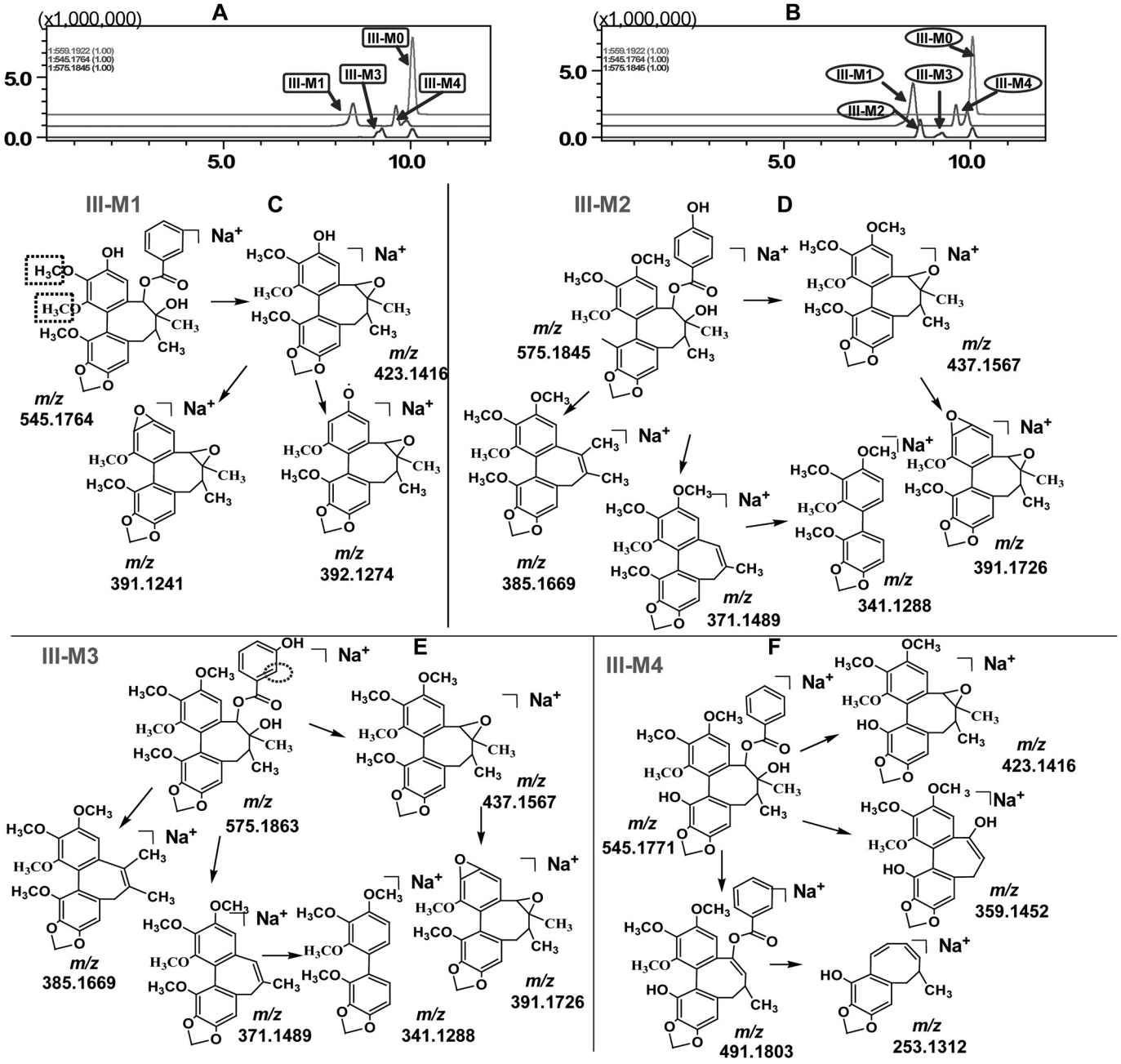

FIG. 5. EICs of schisantherin A and their metabolites in female (A) and male (B) rat liver S9 in the presence of NADPH measured by LC-IT-TOF/MS, and the fragmentation pathways of the possible metabolites of schisantherin A (C–F). Dotted square: the potential demethylation site.

In conclusion, the major metabolic pathways for all of these five lignans were summed as demethylation ($-CH_3$), hydroxylation ($+OH$), and demethylation and hydroxylation ($-CH_3$ and $+OH$). In addition, a great difference in metabolism has been found between female and male rats. In female rats, the major metabolic pathways were demethylation and hydroxylation, and the demethylate and hydroxylate ($-CH_3$ and $+OH$) metabolite was not found. In contrast, the intensities of the metabolites formed by demethylation and hydroxylation ($-CH_3$ and $+OH$) was found to be much higher than the other metabolites. The probability of the metabolic pathways for *Schisandra* lignans was calculated according to the abundances of the metabolites in female and male rat liver S9 (illustrated in Fig. 8).

Phase I Metabolites of Five Major Lignans in Female and Male Intestinal S9 System (Step 2). Schizandrol A and B, schizandrin A and B, and schisantherin A (20 μM) were also incubated both in the presence and absence of the NADPH-generating system with female and male rat intestinal S9 fractions. In the presence of both rat intestinal S9 and NADPH, LC-IT-TOF/MS analysis indicated that most of the metabolites produced in rat liver S9 system were also detected in rat intestinal S9 system. However, the amount of the metabolites was far less than that in rat liver S9 system.

Taking schizandrol A as an example, the four metabolites that appeared in the rat liver S9 system were also detected in female and male intestinal liver S9 supplemented with NADPH. In comparisons between genders, the peak area of these metabolites and the parent drug in female intestinal S9 were similar to those in males. In addition to II-M1, the other five metabolites that appeared in rat liver S9 system were also detected in intestinal S9 when schizandrol B was

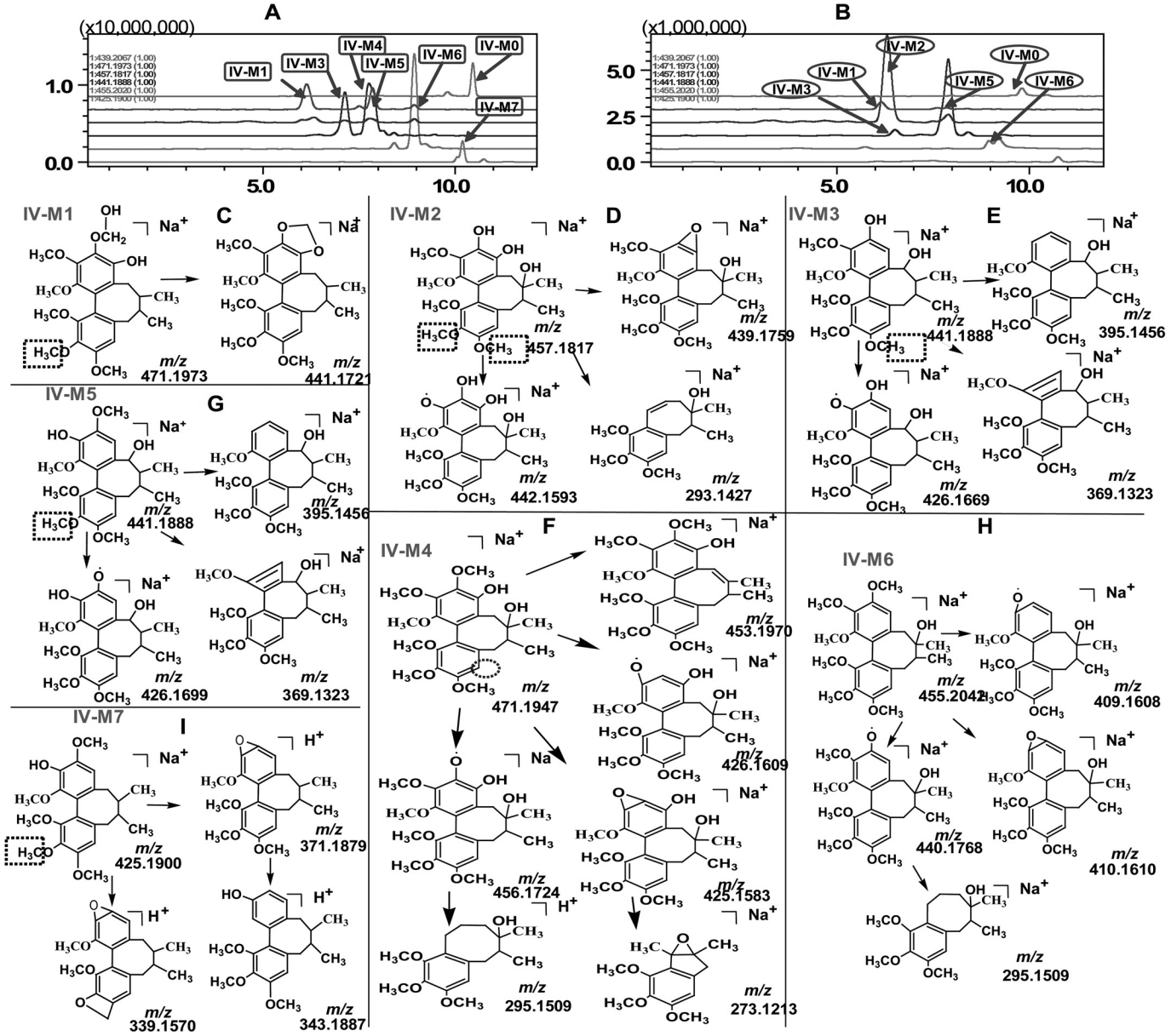

FIG. 6. EICs of schizandrin A and their metabolites in female (A) and male (B) rat liver S9 in the presence of NADPH measured by LC-IT-TOF/MS, and the fragmentation pathways of the possible metabolites of schizandrin A (C–I).

incubated with rat intestinal S9 supplemented with NADPH. As a result, the amount of these metabolites in female and male rats was not significantly different. When schisantherin A was incubated with rat intestinal S9 in presence of NADPH, all four metabolites that appeared in rat liver S9 system were detected, although the amount of III-M2 and III-M3 was close to the limit of quantification. After incubating schizandrin A with female and male rat intestinal S9 in the presence of NADPH, only two metabolites (IV-M3 and IV-M3) were detected, and the amount was far less than that in rat liver S9 system. In addition to V-M1, the other six metabolites that appeared in rat liver S9 system were also detected in intestinal S9 when schizandrin B was incubated with rat intestinal S9 supplemented with NADPH. Likewise, the amount of these metabolites in female and male rats was not significantly different.

Identify and Classify Metabolites for SLE in Rat Urine (Steps 3 and 4). Rat urine collected at 0, 0 to 12, 12 to 24, and 24 to 48 h after an intragastric administration of SLE (500 mg/kg) was used to identify the potential metabolites of lignan components. The LC separation was carried under GEM2 mode because the components to be separated were very complex, and the eluate from HPLC was analyzed by IT-TOF mass spectrometry. The positive mode gave $[M+H]^+$ and/or $[M+Na]^+$ as pseudo-molecular ions, whereas there was no signal detected in the negative ion scan mode. All of these ions were subjected to up to MS^3 experiments, and two collision energies at 50 and 100% were applied to all precursor ions fragmentations to generate sufficient product ions effectively.

In this process, a simple five-step approach was developed to facilitate the identification of metabolites in rat urine. First, we established a database of metabolites based on the metabolic rules of the five lignans in vitro and the exact *m/z* of 31 lignans in SLE. Second step, the endogenous interferences were rapidly excluded by comparing the mass profiles of the dosed urine samples with that of the blank rat urine using Profiling software (Shimadzu). Third, the parent lignans components in urine were readily characterized by comparing

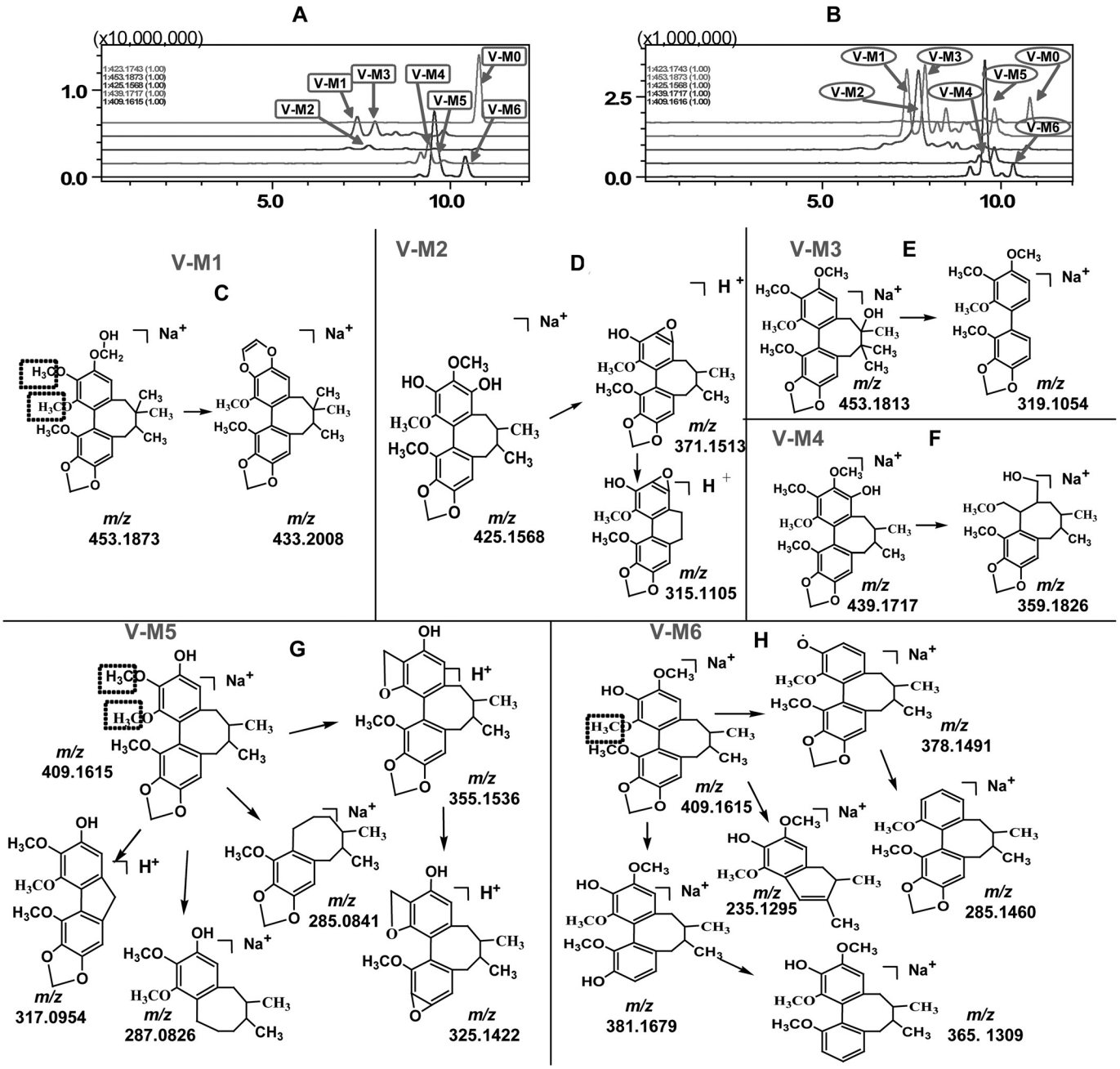

FIG. 7. EICs of schizandrin B and their metabolites in female (A) and male (B) rat liver S9 in the presence of NADPH measured by LC-IT-TOF/MS, and the fragmentation pathways of the possible metabolites of schizandrin B (C–H). Dotted square: the potential demethylation site.

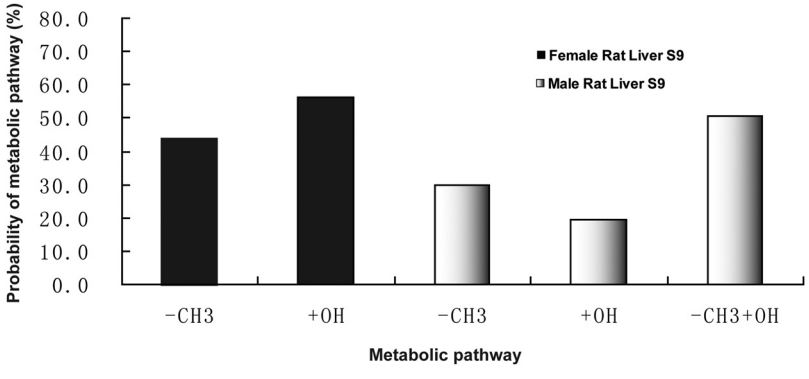

FIG. 8. The probability of the metabolic pathways for *Schisandra* lignans calculated according to the abundances of the metabolites in female and male rats liver S9.

the mass profiles of urine samples after SLE dosage with that of SLE per se. Fourth step, the remaining peaks in the dosed urine after the second and third step of exclusions were treated as potential metabolites, and we could calculate the formula according to the exact *m/z* of these potential metabolites. Finally, the metabolites were classified by comparing the formula proposed in the first step with those calculated in the fourth step. The results of the classification could be further validated according to their retention time and accurate MS/MS^n.

The in vitro metabolism of five representative lignans in SLE had been studied, and intestinal S9 and demethylation ($-CH_3$), hydroxylation ($+OH$), and demethylation-hydroxylation ($-CH_3+OH$) were identified as the primary metabolic pathways. Tentatively, at least 93 metabolites could be inferred easily based on the above studies, and the empirical formula for these parent lignans and their potential metabolites were calculated and listed in a formula library established by the author. After comparing the mass spectra of dosed urine samples with that of the blank rat urine by Profiling software (Shimadzu), 62 lignan compounds were detected in the dosed urine samples of male and female rats. Then, these lignan compounds in the dosed urine samples were compared with constitute of SLE per se, and 18 compounds in female and male rat urine were confirmed as parent compounds. Forty-four metabolites were found in rat urine (data shown in Fig. 9). The formula of these nontargeted metabolites were calculated by Formula Predictor software (Shimadzu) according to their exact *m/z* determined by LC-IT-TOF/MS (data shown in Supplemental Table S1) and then matched with those in the formula library established previously. In this procedure, most of the potential metabolites were classified because their corresponding parent compounds were identified and the metabolic pathways were proposed. These metabolites were further verified according to their retention time and fragment ions, and the detailed MS^n information had been shown in Table S1, and nearly all the mass errors of MS and MS^n were <5 ppm. As seen in Table 2, 20 hydroxylated and seven demethylated metabolites were classified in this process. Eight demethylated- hydroxylated metabolites were also located in both male and female rat urine. More importantly, these biotransformations were found to occur on gomisin O/epigomisin O, gomisin T-ol, schizandrol A, schizandrol B, tigloyl/angeloylgomisin H, tigloyl/angeloylgomisin P, angeloylgomisin Q, gomisin D, gomisin F, schisantherin C, and schisantherin B. M21 (*m/z* 541.1824), eluted at 10.6 min, was tentatively identified as a hydrate metabolite of tigloyl/angeloylgomisin H. M27 (*m/z* 553.2408) and M37 (*m/z* 567.1956) were identified as methylated-hydroxylated metabolites of tigloyl/angeloylgomisin H and schisantherin C, respectively.

Glucuronidation experiments were also conducted by incubating schizandrol A and B, schizandrin A and B, and schisantherin A with S9 (either liver or intestinal) together with saccharolactone (5 mM, final concentration) and magnesium chloride (1 mM, final concentration) at a protein concentration of 1 mg/ml, respectively. To start the reaction, UDP-glucuronic acid [(UDPGA) 5 mM, final concentration] was added and the final volume of the reaction mixture was 200 μl. As a result, the relative intensities of schizandrol A and B, schizandrin A and B, and schisantherin A in the presence of the UDPGA-generating system were similar to those in the absence of the UDPGA-generating system, and no glucuronide conjugate was observed in these in vitro incubations. Three glucuronide conjugates (M42, M43, and M44) were observed in male rat urine, and M45 was also observed in female rat urine. M42, eluted at 4.3 min, exhibited a molecular ion at *m/z* 617.2059 in the positive ESI MS spectrum. In the MS/MS/CID experiment, one major product ion at *m/z* 441.1882 ($C_{23}H_{30}O_7$) was formed by a neutral loss of 176.0196, which suggests that glucuronidation had occurred in this metabolic process. After comparing the formula of this fragment with that of lignans in SLE, we identified the parent compound of M42 as gomisin or gomisin T-ol because their formula ($C_{23}H_{30}O_7$) could match perfectly with that of the product ion (*m/z* 441.1882). Likewise, the formula of metabolite M43 was calculated as $C_{28}H_{36}O_{14}$ by the Formula Predictor software according to the accurate mass measurements (*m/z* 619.1933), and the LC retention time was approximately 4.1 min. The fragment ion at *m/z* 443.1682 ($C_{22}H_{28}O_8$) resulted from the loss of a glucuronide moiety as a neutral fragment, and this metabolite was identified as glucuronide conjugate of demethylated-hydroxylated gomisin and/or gomisin T-ol. M44, eluted at 3.9 min, was calculated as $C_{29}H_{42}O_{14}$ by the Formula Predictor software according to the accurate mass measurements (*m/z* 633.2111) and appeared in both female and male rat urine. Based on the approach stated above, this metabolite was confirmed as the demethylated-hydroxylated schizandrol A. In addition, we also tried many ways to search for sulfate metabolites in in vitro and in vivo systems; however, no single sulfate metabolites were observed in the rat urine and the liver/intestinal S9 sulfation metabolic systems.

Gender differences were also investigated according to the cumulative excretion of the 44 metabolites. In this procedure, RCE was calculated by numeric integration of the amount (peak area of EICs*Volume) excreted per collection interval (0–12, 12–24, and 24–48 h). As a result, great gender-related differences on RCE were observed. For most metabolites, RCE in female rats was significantly lower than that in male rats (illustrated in Fig. 10).

Discussion

Herbal medicine is always defined as a therapeutic regimen that, rather than consisting of a single compound that interacts with a single target, is a concerted pharmacological intervention of several compounds that interact with multiple targets (Arteaga, 2003; Kong et al., 2008). Due to the diverse biological activities and medicinal potentials of natural products, nearly every civilization has accumulated experience and knowledge of their use (Pomeranz and Warma, 1988; Rackley et al., 2006). More recently, Western pharmaceutical companies quickly began to prefer purified natural products as ingredients to make drugs rather than crude extracts (Yuan and Lin, 2000; Li and Zhang, 2008). Nevertheless, there is a huge challenge in identifying natural compounds or naturally inspired compounds that can be combined to be effective against disease. In addition, the enormous number of possible metabolites in vivo, the inherent risks of harmful drug-drug interactions, and the unpredictable pharmacokinetic properties of multicomponent formulations must still be addressed. As pointed out above, the metabolic research for herbal medicine is not only critical to the modernization of HM per se, but it is also important to the development of new drugs.

However, metabolic study for herbal medicine is a formidable task due to the following challenges: 1) HM is a complex system because, in most cases, medicinal plants comprise hundreds of different constituents with diverse chemical and physical properties; 2) it is very difficult to classify the metabolites due to complex metabolic pathways and various parent compounds; 3) most of components are unknown (nontarget); 4) the lack of authentic reference standards constituents is another great and longstanding obstacle in charactering herbal metabolism; and 5) it is very feasible to prepare the metabolites by preparative HPLC because the good separation for such complex components is almost impossible.

The present study contributes to the development of a systematic methodology in addressing the critical problems underlined in the

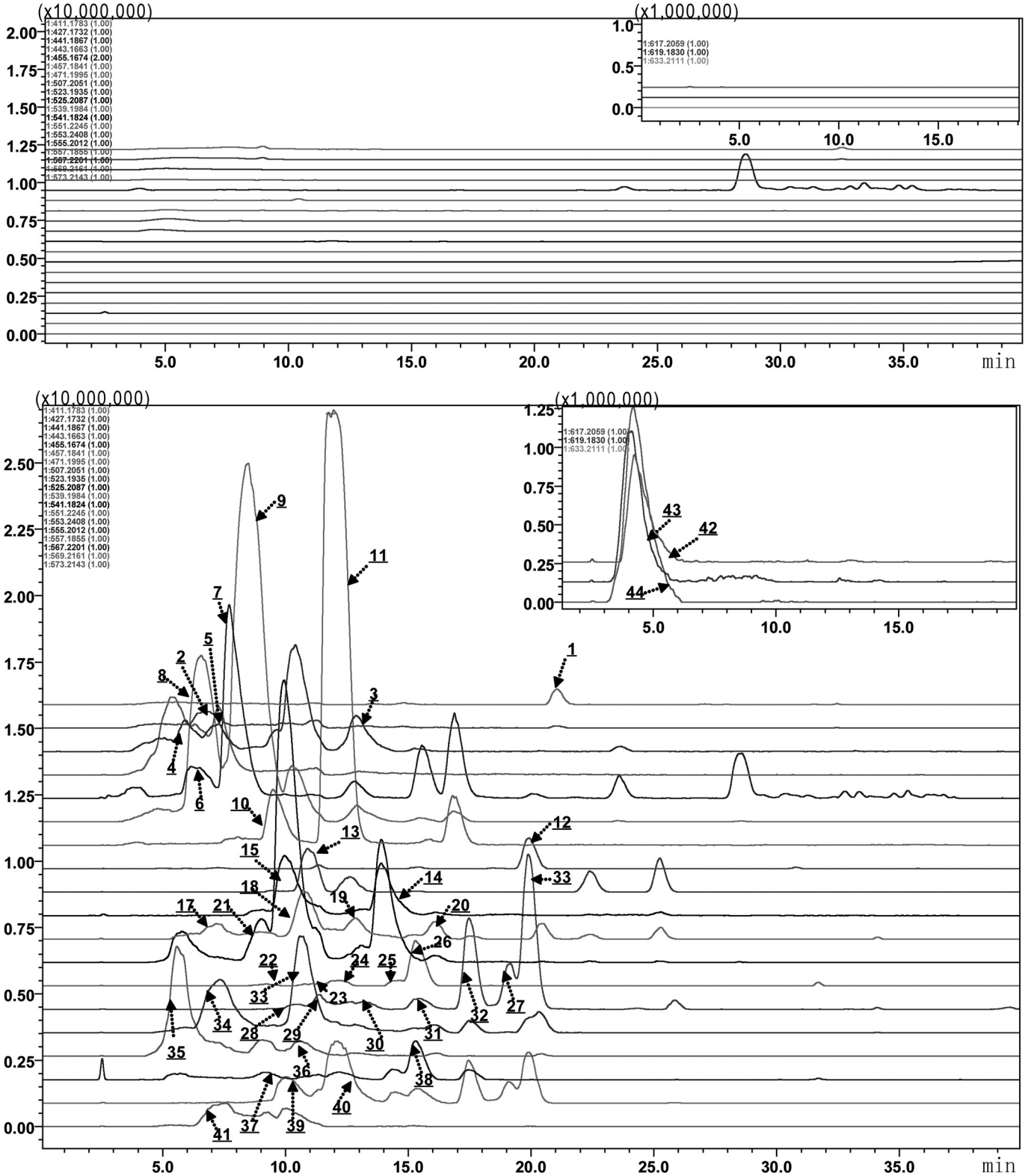

FIG. 9. EICs of a blank urine sample and a dosed urine sample collected from male rats. Top, blank urine of a male rat; Bottom, male rat urine collected during 0 to 12 h after dosing SLE at 500 mg/kg.

field of herbal metabolism, including the identification and classification of metabolites, based on a single LC-IT-TOF/MS platform (Fig. 11). Herein, the proposed systematic mythology based on LC-IT-TOF/MS platform was successfully used to indentify and classify the metabolites for *Schisandra* lignans. First, diagnostic fragment-ion-based extension strategy was used for the rapid identification of lignans in SLE, and 31 kinds of lignans were structurally characterized in this process. Second, the metabolic fate for five major lignan components with authentic standards was studied one by one in liver and intestinal S9 systems according to the accurate mass measurement

TABLE 2

The metabolites of SLE in female and male rat urine

Mets	*m/z* [M + Na]$^+$	t_R (min)	Parent Compounds	Biotransformation	Mets	*m/z* [M + Na]$^+$	t_R (min)	Parent Compounds	Biotransformation
1	411.1783	21.2	Gomisin O/epigomisin O	−CH3	23	551.2059	11.3	Schisantherin C	+OH-2H
2	427.1732	7.5	Gomisin T-ol	−CH3	24	551.2045	12.1	Schisantherin B	+OH-2H
3	441.1867	13.8	Schizandrol A	−CH3	25	551.2059	14.3	Tigloyl/angeloylgomisin P	+OH-2H
4	443.1663	7.8	Gomisin T-ol	−CH3 + OH	26	551.2037	15.4	Tigloyl/angeloylgomisin P	+OH-2H
5	443.166	4.3	Gomisin T-ol	−CH3 + OH	27	553.2408	19.1	Tigloyl/angeloylgomisin H	+CH3 + OH
6	455.1674	7.7	Schizandrol B	+OH	28	553.2071	10.4	Gomisin F	+OH
7	455.1665	8.6	Schizandrol B	+OH	29	553.2071	11.6	Schisantherin C	+OH
8	457.1841	6.3	Gomisin T-ol	+OH	30	553.2071	12.6	Schisantherin B	+OH
9	457.1841	8.6	Schizandrol A	−CH3 + OH	31	553.2071	13.2	Tigloyl/angeloylgomisin P	+OH
10	471.1995	11.9	Schizandrol A	+OH	32	553.2071	15.5	Tigloyl/angeloylgomisin P	+OH
11	471.1957	8.9	Schizandrin A	+2OH	33	555.2012	10.7	Gomisin D	−CH3 + OH
12	507.2051	20.0	Tigloyl/angeloylgomisin H	−CH3	34	555.2219	7.0	Angeloylgomisin Q	−CH3 + OH
13	523.1935	11.1	Tigloyl/angeloylgomisin P	−CH3	35	557.1855	8.5	Gomisin G	−2H
14	525.2087	14.0	Tigloyl/Angeloylgomisin H	−CH3 + OH	36	557.1884	10.3	Schisantherin A	−2H
15	525.2105	10.0	Tigloyl/angeloylgomisin H	−CH3 + OH	37	567.1956	9.1	Schisantherin C	+CH3 + OH
16	539.2254	20.3	Angeloylgomisin Q	−CH3	38	567.2201	17.5	Angeloylgomisin Q	+OH-2H
17	539.1984	15.8	Gomisin D	−CH3	39	569.2161	10.1	Gomisin D	+OH
18	539.2249	12.6	Tigloyl/angeloylgomisin H	+OH	40	569.2161	11.9	Angeloylgomisin Q	+OH
19	539.2239	10.7	Tigloyl/angeloylgomisin H	+OH	41	573.2143	9.0	Schisantherin A	+OH-2H
20	539.1984	7.4	Tigloyl/angeloylgomisin P	−CH3 + OH	42	617.2059	4.3	Gomisin T-ol/gomisin	+GLU
21	541.1824	10.6	Tigloyl/angeloylgomisin H	+H2O	43	619.1830	4.1	Gomisin T-ol	−CH3 + OH + GLU
22	551.2045	8.9	Gomisin F	+OH-2H	44	633.2111	3.9	Schizandrol A	−CH3 + OH + GLU

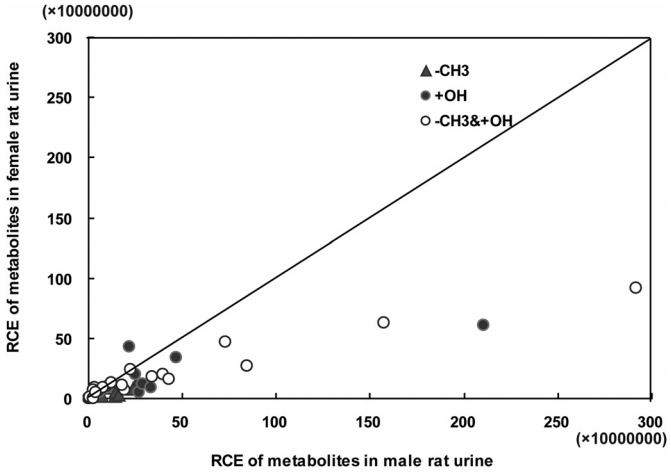

FIG. 10. Gender-related difference in liver S9 on RCE.

for MS and MS^n based on LC-IT-TOF/MS. The primary biotransformation, including demethylation (−CH_3), hydroxylation (+OH), and demethylation-hydroxylation (−CH_3+OH) were summarized for schizandrol A and B, schizandrin A and B, and schisantherin A. In

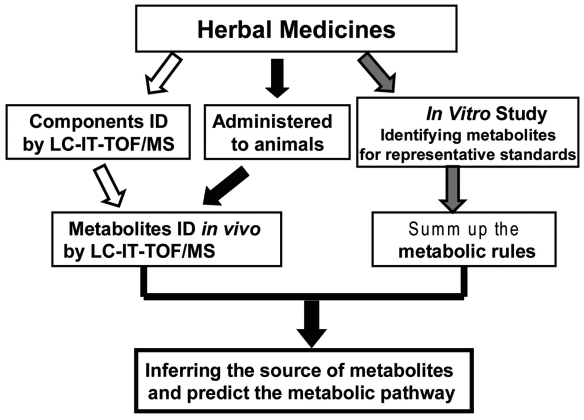

FIG. 11. Suggested herbal metabolism platform and workflow based on LC-IT-TOF/MS.

general, the metabolic research in vivo and in vitro was in high correlation, and the diversity of lignans in SLE was multiplied by the composition of methyl and hydroxyl numbers, branching patterns, and the type of substitution (Huang et al., 2008; Lu and Chen, 2009). Thus, the metabolites in vivo for the 31 lignans could be easily traced based on the metabolic pathways of the known lignan standards. Finally, there are dozens of metabolites predicted that were not detected in rat urine. The main reasons for this could be summed up as follows: 1) there was a large dynamic range of concentration scales for the parent compounds in SLE; 2) to some extent, metabolic capabilities have differences for different lignans; and 3) the concentrations of several metabolites were below the lowest limits of detection. In addition, several metabolites, e.g., hydration and methylation metabolites, could not be detected in vitro but were found in vivo. This result was certainly due to the more complex types of metabolic enzymes in vivo rather than those in vitro.

Gender difference in pharmacokinetics characterizes many drugs and contribute to individual differences in drug efficacy and toxicity (Fletcher et al., 1994; Franconi et al., 2007). Gender-based differences in drug metabolism are the primary cause of sex-dependent pharmacokinetics and reflect underlying sex differences in the expression of hepatic enzymes active in the metabolism of drugs, steroids, fatty acids, and environmental chemicals, including cytochromes P450 (P450s), sulfotransferases, glutathione transferases, and UDP-glucuronosyltransferases (Pierce et al., 2009). Studies in the rat and mouse liver models have identified more than 1000 genes whose expression is sex-dependent; together, these genes impart substantial sexual dimorphism to liver metabolic function and pathophysiology (Yang et al., 2006; Chouinard et al., 2008; Wauthier and Waxman, 2008). In this work, the peak area of the parent compounds in female rat liver S9 system was found to be much higher than that in male rat liver S9 system after incubating schizandrol A and B and schizandrin A and B with rat liver S9 in the presence of the NADPH-generating system. In this procedure, gender difference was also found in both the type and the relative amount of metabolites. In the subsequent in vivo experiments, a RCE, calculated by numeric integration of the amount (peak area of EICs*Volume) excreted per collection interval (0–6, 6–12, 12–24, and 24–48 h), was developed to assess the relative amount of each metabolite in male and female rat urine independent of specific

authentic compounds. As a result, great gender-related differences on RCE were observed. For most metabolites, RCE in female rats was significantly lower than that in male rats. These results are consistent with numerous previous studies, which showed that most of the enzyme activities in liver microsomes of male rats were 1.5- to 5-fold higher than that of female rats (Ryuichi and James, 1965; Theodore et al., 1970; Waxman and Holloway, 2009). Sex-dependent, hepatic P450s in the rat are generally divided into three groups: 1) male-specific isoforms only found in male liver, 2) female-specific isoforms only expressed in female liver, and 3) female-predominant P450s found in both sexes but at higher levels in females (Morgan et al., 1985; Thangavel et al., 2006). Essentially, there are four major male-specific isoforms in rat liver: CYP2C11, CYP2C13, CYP2A2, and CYP3A2. From the metabolites in urine, demethylation ($-CH_3$), hydroxylation ($+OH$) and demethylation-hydroxylation had occurred on gomisin O/epigomisin O, gomisin T-ol, schizandrol A, schizandrol B, tigloyl/angeloylgomisin H, tigloyl/angeloylgomisin P, angeloylgomisin Q, gomisin D, gomisin F, schisantherin C, and schisantherin B. Iwata et al. (2004) and Lai et al. (2010) had reported that Schisandra lignans were the potent CYP3A4, CYP1A2, CYP2C9, CYP2C19, and CYP2D6 inhibitors. Until now, the specific enzyme types, which were responsible for metabolizing Schisandra lignans, were not identified clearly.

References

Arteaga CL (2003) Molecular therapeutics: is one promiscuous drug against multiple targets better than combinations of molecule-specific drugs? *Clin Cancer Res* **9:**1231–1232.

Bradford MM (1976) A rapid and sensitive method for the quantitation of microgram quantities of protein utilizing the principle of protein-dye binding. *Anal Biochem* **72:**248–254.

Chouinard S, Yueh MF, Tukey RH, Giton F, Fiet J, Pelletier G, Barbier O, and Bélanger A (2008) Inactivation by UDP-glucuronosyltransferase enzymes: the end of androgen signaling. *J Steroid Biochem Mol Biol* **109:**247–253.

Curiati JA, Bocchi E, Freire JO, Arantes AC, Braga M, Garcia Y, Guimarães G, and Fo WJ (2005) Meditation reduces sympathetic activation and improves the quality of life in elderly patients with optimally treated heart failure: a prospective randomized study. *J Altern Complement Med* **11:**465–472.

Deng X, Chen X, Yin R, Shen Z, Qiao L, and Bi K (2008) Determination of deoxyschizandrin in rat plasma by LC-MS. *J Pharm Biomed Anal* **46:**121–126.

Engel LW and Straus SE (2002) Development of therapeutics: opportunities within complementary and alternative medicine. *Nat Rev Drug Discov* **1:**229–237.

Fletcher CV, Acosta EP, and Strykowski JM (1994) Gender differences in human pharmacokinetics and pharmacodynamics. *J Adolesc Health* **15:**619–629.

Franconi F, Brunelleschi S, Steardo L, and Cuomo V (2007) Gender differences in drug responses. *Pharmacol Res* **55:**81–95.

Goldrosen MH and Straus SE (2004) Complementary and alternative medicine: assessing the evidence for immunological benefits. *Nat Rev Immunol* **4:**912–921.

Hao H, Cui N, Wang G, Xiang B, Liang Y, Xu X, Zhang H, Yang J, Zheng C, Wu L, et al. (2008) Global detection and identification of nontarget components from herbal preparations by liquid chromatography hybrid ion trap time-of-flight mass spectrometry and a strategy. *Anal Chem* **80:**8187–8194.

Huang X, Song F, Liu Z, and Liu S (2008) Structural characterization and identification of dibenzocyclooctadiene lignans in Fructus Schisandrae using electrospray ionization ion trap multiple-stage tandem mass spectrometry and electrospray ionization Fourier transform ion cyclotron resonance multiple-stage tandem mass spectrometry. *Analytica chimica acta* **615:**124–135.

Huang XD, Kong L, Li X, Chen XG, Guo M, and Zou HF (2004) Strategy for analysis and screening of bioactive compounds in traditional Chinese medicines. *J Chromatogr B Analyt Technol Biomed Life Sci* **812:**71–84.

Institute of Laboratory Animal Resources (1996) *Guide for the Care and Use of Laboratory Animals* 7th ed. Institute of Laboratory Animal Resources, Commission on Life Sciences, National Research Council, Washington DC.

Iwata H, Tezuka Y, Kadota S, Hiratsuka A, and Watabe T (2004) Identification and characterization of potent CYP3A4 inhibitors in Schisandra fruit extract. *Drug Metab Dispos* **32:**1351–1358.

Jiang Y, David B, Tu P, and Barbin Y (2010) Recent analytical approaches in quality control of traditional Chinese medicines–a review. *Anal Chim Acta* **657:**9–18.

Kong DX, Li XJ, Tang GY, and Zhang HY (2008) How many traditional Chinese medicine components have been recognized by modern Western medicine? A chemoinformatic analysis and implications for finding multicomponent drugs. *Chem Med Chem* **3:**233–236.

Lai L, Hao HP, Wang Q, Zheng CN, Zhou F, Liu YT, Wang YX, Yu G, Kang A, Peng Y, et al. (2009) Effects of short-term and long-term pretreatment of Schisandra lignans on regulating hepatic and intestinal CYP3A in rats. *Drug Metab Dispos* **37:**2399–2407.

Li XJ and Zhang HY (2008) Synergy in natural medicines: implications for drug discovery. *Trends Pharmacol Sci* **29:**331–332.

Lu Y and Chen DF (2009) Analysis of Schisandra chinensis and Schisandra sphenanthera. *J Chromatogr A* **1216:**1980–1990.

Masaki K, Hashimoto M, and Imai T (2007) Intestinal first-pass metabolism via carboxylesterase in rat jejunum and ileum. *Drug Metab Dispos* **35:**1089–1095.

Morgan ET, MacGeoch C, and Gustafsson JA (1985) Hormonal and developmental regulation of expression of the hepatic microsomal steroid 16α-hydroxylase cytochrome P-450 apoprotein in the rat. *J Biol Chem* **260:**11895–11898.

Mori Y, Yamazaki H, Toyoshi K, Denda A, and Konishi Y (1986) Mutagenic activation of carcinogenic N-nitrosopropylamines by liver S9 factions from mice, rats and hamsters: evidence for a cytochrome P450-dependent reaction. *Carcinogenesis* **7:**375–379.

Pierce JP, Kievits J, Graustein B, Speth RC, Iadecola C, and Milner TA (2009) Sex differences in the subcellular distribution of angiotensin type 1 receptors and NADPH oxidase subunits in the dendrites of C1 neurons in the rat rostral ventrolateral medulla. *Neuroscience* **163:**329–338.

Pomeranz B and Warma N (1988) Electroacupuncture suppression of a nociceptive reflex is potentiated by two repeated electroacupuncture treatments: the first opioid effect potentiates a second non-opioid effect. *Brain Res* **452:**232–236.

Rackley JD, Clark PE, and Hall MC (2006) Complementary and alternative medicine for advanced prostate cancer. *Urol Clin North Am* **33:**237–246, viii.

Ryuichi K and James RG (1965) Effect of starvation on NADPH-dependent enzymes in liver microsomes of male and female rats. *J Pharmacol Exp Ther* **2:**279–284.

Thangavel C, Dworakowski W, and Shapiro BH (2006) Inducibility of male-specific isoforms of cytochrome P450 by sex-dependent growth hormone profiles in hepatocyte cultures from male but not female rats. *Drug Metab Dispos* **34:**410–419.

Theodore EG, Anthony MG, David HS, Donald CD, Reginald LR, and James RG (1970) The effect of starvation on the kinetics of drug oxidation by hepatic microsomal enzymes from male and female rats. *J Pharmacol Exp Ther* **1:**12–21.

VandenBranden M, Wrighton SA, Ekins S, Gillespie JS, Binkley SN, Ring BJ, Gadberry MG, Mullins DC, Strom SC, and Jensen CB (1998) Alterations in the catalytic activities of drug-metabolizing enzymes in cultures of human liver slices. *Drug Metab Dispos* **26:**1063–1068.

Vickers AE, Connors S, Zollinger M, Biggi WA, Larrauri A, Vogelaar JP, and Brendel K (1993) The biotransformation of the ergot derivative CQA 206–291 in human, dog, and rat liver slice cultures and prediction of in vivo plasma clearance. *Drug Metab Dispos* **21:**454–459.

Wang Y, Hao H, Wang G, Tu P, Jiang Y, Liang Y, Dai L, Yang H, Lai L, Zheng C, et al. (2009) An approach to identifying sequential metabolites of a typical phenylethanoid glycoside, echinacoside, based on liquid chromatography-ion trap-time of flight mass spectrometry analysis. *Talanta* **80:**572–580.

Wauthier V and Waxman DJ (2008) Sex-specific early growth hormone response genes in rat liver. *Mol Endocrinol* **22:**1962–1974.

Waxman DJ and Holloway MG (2009) Sex differences in the expression of hepatic drug metabolizing enzymes. *Mol Pharmacol* **76:**215–228.

Xu MJ, Wang GJ, Xie HT, Huang Q, Wang W, and Jia YW (2008) Pharmacokinetic comparisons of schizandrin after oral administration of schizandrin monomer, Fructus Schisandrae aqueous extract and Sheng-Mai-San to rats. *J Ethnopharmacol* **115:**483–488.

Yang M, Sun J, Lu Z, Chen G, Guan S, Liu X, Jiang B, Ye M, and Guo DA (2009) Phytochemical analysis of traditional Chinese medicine using liquid chromatography coupled with mass spectrometry. *J Chromatogr A* **1216:**2045–2062.

Yang X, Schadt EE, Wang S, Wang H, Arnold AP, Ingram-Drake L, Drake TA, and Lusis AJ (2006) Tissue-specific expression and regulation of sexually dimorphic genes in mice. *Genome Res* **16:**995–1004.

Yuan R and Lin Y (2000) Traditional Chinese medicine: an approach to scientific proof and clinical validation. *Pharmacol Ther* **86:**191–198.

Zheng C, Hao H, Wang X, Wu X, Wang G, Sang G, Liang Y, Xie L, Xia C, and Yao X (2009) Diagnostic fragment-ion-based extension strategy for rapid screening and identification of serial components of homologous families contained in traditional Chinese medicine prescription using high-resolution LC-ESI-IT-TOF/MS: Shengmai injection as an example. *J Mass Spectrom* **44:**230–244.

Address correspondence to: Professor Guangji Wang, Key Laboratory of Drug Metabolism and Pharmacokinetics, China Pharmaceutical University, Nanjing 210009, People's Republic of China. E-mail: guangjiwang@hotmail.com